

# Technical Notes

TECHNICAL NOTES are short manuscripts describing new developments or important results of a preliminary nature. These Notes cannot exceed 6 manuscript pages and 3 figures; a page of text may be substituted for a figure and vice versa. After informal review by the editors, they may be published within a few months of the date of receipt. Style requirements are the same as for regular contributions (see inside back cover).

## Real Gas Effect in a Laser Heated Thruster

Peter K. Wu\*

Physical Sciences Inc., Woburn, Mass.

### Introduction

WHEN a laser beam is focused in air with a flux greater than  $10^4$  W/cm<sup>2</sup>, a heated zone has been observed to propagate up the beam at either subsonic<sup>1,2</sup> or supersonic<sup>3</sup> velocities. The subsonic mode, a laser supported combustion (LSC) wave, is analogous to the burning of a combustible mixture. The zone heats the adjacent regions by conduction and radiation to a high enough temperature to ionize the air which then becomes opaque to the laser radiation. As the laser flux is increased to  $\geq 10^7$  W/cm<sup>2</sup>, the rapid energy deposition causes the shock-heating of the adjacent regions to a high temperature, and this becomes the laser supported detonation wave. Since we are considering a thruster with the laser beam from the upstream parallel to the flow, the plasma formed in the nozzle will also tend to propagate up the laser beam in this manner. Therefore, in order to maintain a stationary plasma in the subsonic section of the nozzle, the flow velocity at the plasma location must be equal and opposite to the propagation velocity of the plasma. Hence, we are primarily interested in the propagation of LSC waves.

Experimental data for the propagation of LSC waves exist mostly for air, and models for their propagation have been developed in Refs. 4-6. Here, we chose to apply the Jackson model for the propagation of an LSC wave in hydrogen because of its simplicity, and the selection of hydrogen has been based on the specific impulse consideration. However there are uncertainties associated with this model. The ignition temperature ( $T_i$ ) (temperature at which the air begins to absorb significantly) is an *a priori* assumed parameter which is estimated from the absorption characteristics of the flowing gas. In addition, the experimental data for the propagation velocity in air are approximately a factor of 3.5 above the theoretical values (Fig. 1). Nevertheless, in practice, one can compensate for this uncertainty in the propagation velocity by varying the focusing angle of the laser beam or the nozzle inlet flow velocity.

Applying this model to hydrogen, we have to make some further assumptions about the characteristic of the absorption and emission of radiation by hydrogen at high temperatures. The cold hydrogen in front of the heated zone is assumed to be heated first by conduction from the heated zone to raise the temperature, and hence the concentration of hydrogen atoms which absorb radiation from the hot plasma. A classical continuous absorption coefficient is assumed.<sup>7</sup> As for the hot plasma, it absorbs the laser radiation by inverse Bremsstrahlung, and its radiated power per unit volume for simplicity is taken from Yos.<sup>8</sup> Shown in Fig. 1 are calculations

carried out for hydrogen at pressures of one and three atm. In these calculations, the ignition temperature has been assumed to be 12,000°K. With the knowledge of propagation velocity as a function of the laser flux, we can now proceed to carry out flow field analysis downstream of the wave to determine the thermodynamic properties and nozzle size as a function of laser power.

### Method of Analysis

The one-dimensional steady nozzle flow with laser energy addition has been previously studied.<sup>9</sup> The flow was considered to be that of a perfect gas, and the absorbed laser energy was assumed to be instantaneously converted to temperature (i.e., equilibrium flow). However, the hydrogen is completely dissociated at about 5000°K (for  $p=1$  atm) and ionization becomes important at  $T \sim 14,000^\circ\text{K}$ . With the temperature in the heated zone greater than 12,000°K, the ideal gas assumptions can introduce significant errors. Here, we will assess the real gas effects on the thermodynamic properties in a laser-heated nozzle. The governing equations are the continuity, momentum, and energy equations, and the equation of state. In addition, one defines a sound speed  $a^2 = \gamma RT/W$  and a Mach number  $M^2 = u^2/a^2$ . Now, we have six equations for six unknowns,  $\rho$ ,  $u$ ,  $p$ ,  $T$ ,  $A$ , and  $M$ . The above equations can be written in the differential forms, and after some algebra, we have

$$\frac{I}{M^2} \frac{dM^2}{d\tau} = [I - g_1] \frac{I}{W} \frac{dW}{d\tau} - \frac{I}{\gamma} \frac{d\gamma}{d\tau} + [g_1 - I] \frac{dQ/d\tau + dh_p/d\tau}{c_p T} - \frac{g_1}{A} \frac{dA}{d\tau} \quad (1)$$

$$\frac{I}{T} \frac{dT}{d\tau} = [I - g_2] \frac{I}{W} \frac{dW}{d\tau} + g_2 \frac{dQ/d\tau + dh_p/d\tau}{c_p T} + [I - g_2] \frac{I}{A} \frac{dA}{d\tau} \quad (2)$$

where  $\rho$  is the density;  $p$  is the pressure;  $T$  is the temperature;  $u$  is the velocity;  $A$  is the cross-sectional area;  $dQ$  is the laser energy deposition;  $dh_p$  is the change in enthalpy due to the change in pressure;  $W$  is the molecular weight;  $\gamma$  is the ratio of specific heats;  $c_p$  is the specific heat at constant pressure;  $R$  is the universal gas constant; and

$$g_1 = \frac{I + \frac{\gamma R M^2}{2c_p W}}{\frac{I}{2} - \frac{\gamma M^2}{2} + \frac{\gamma R M^2}{2c_p W}}$$

$$g_2 = \frac{I - \gamma M^2}{I - \gamma M^2 + \frac{\gamma R M^2}{c_p W}}$$

and subjected to the boundary conditions  $T(0) = T_i$  and at the singular point near the throat

$$M = (\gamma - \gamma R/c_p W)^{-1/2}$$

Received Aug. 19, 1976; revision received Sept. 22, 1976. This work was sponsored by Rocketdyne Division, Rockwell International, under Project Manager, J. M. Shoji. The author expresses his appreciation to A. N. Pirri for many helpful discussions.

Index categories: Nozzle and Channel Flow; Radiatively Coupled Flows and Heat Transfer; Lasers.

\*Principal Scientist. Member AIAA.

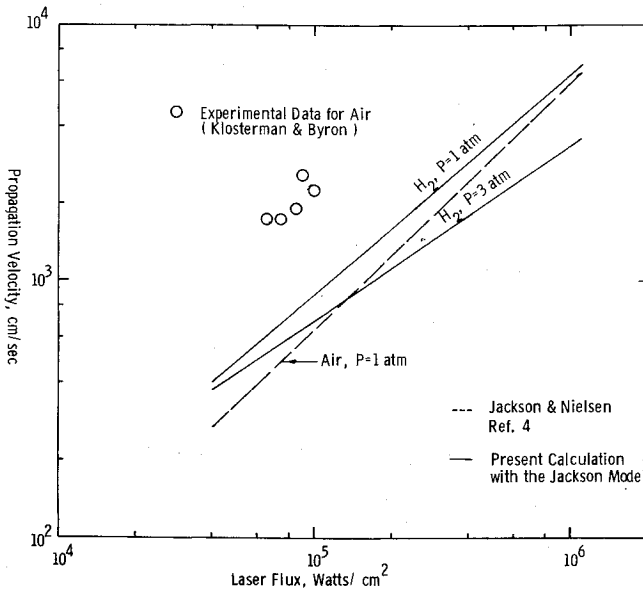
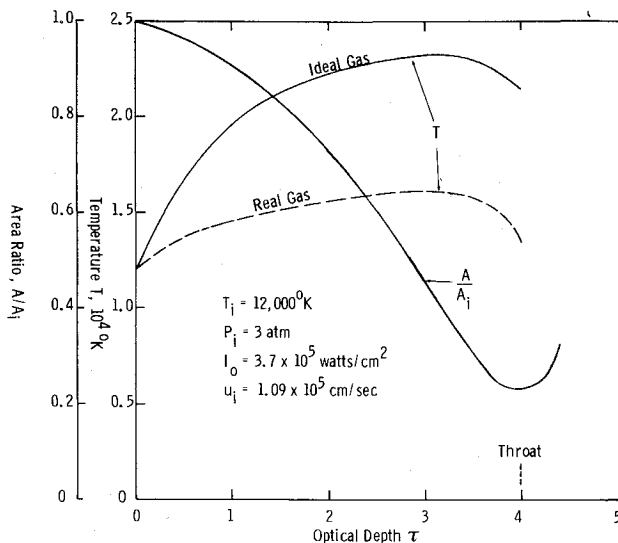


Fig. 1 Laser-supported combustion wave velocity vs laser flux.

Fig. 2 Area ratio and temperature profile vs optical depth  $\tau$ .

The location of the singularity is defined by the expression

$$\frac{1}{c_p T} \left( \frac{dQ}{d\tau} + \frac{dh_p}{d\tau} \right) - \frac{1}{W} \frac{dW}{d\tau} - \frac{1}{A} \frac{dA}{d\tau} = 0$$

The variations of  $\gamma$ ,  $c_p$ ,  $W$ ,  $H$  as function pressure and temperature are obtained from the results of Patch,<sup>10</sup> and are coupled into the calculation explicitly. The optical depth  $\tau$  is defined as

$$\tau = \int_0^x k_\nu dx \quad (3)$$

where  $k_\nu$  is the absorption coefficient. Inserting the previous definition into the radiative transfer equation

$$(d/dx)(IA) = -IA k_\nu$$

We can immediately integrate the resulting equation to obtain the laser power distribution as a function of optical depth  $\tau$ .

$$IA = (IA)_i e^{-\tau}$$

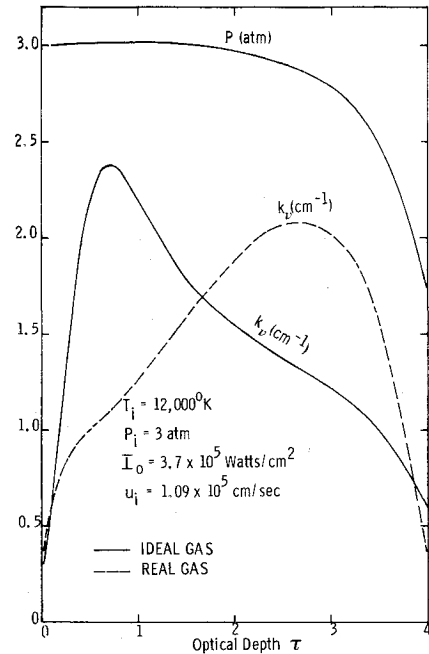
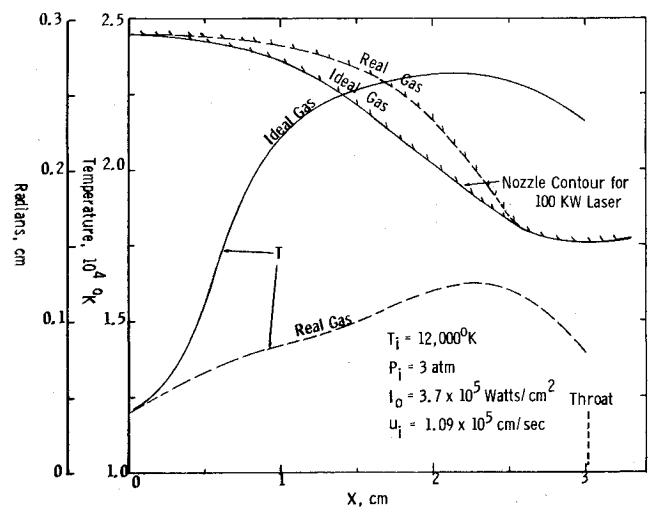
Fig. 3 Pressure profile and absorption coefficient vs optical depth  $\tau$ .

Fig. 4 Nozzle contour for 100 kW laser (radius) and temperature vs distance along nozzle axis.

Hence the laser energy addition  $dQ/d\tau$  becomes

$$dQ/d\tau = (P/\rho u A) e^{-\tau}$$

Finally, for a given nozzle contour  $A$ , we can calculate the Mach number and temperature distributions from Eqs. (1 and 2), and then all other thermodynamic and fluid dynamic properties. The inverse Bremsstrahlung absorption coefficient is given in Ref. 11 as a function of the thermodynamic state of the media. Finally, Eq. (3) enables us to transform the solution into the physical space.

## Results and Discussion

The nozzle calculation can be started anywhere in the nozzle. For simplicity, we choose to start the calculation at a location where the temperature reaches the ignition temperature (the absorption of laser radiation by inverse Bremsstrahlung is also assumed to begin at this point). An example calculation, for  $T_i = 12,000^\circ\text{K}$ ,  $p_i = 3$  atm and  $I_0 = 3.7 \times 10^5 \text{ W/cm}^2$  is shown in Figs. 2-4. With an assumed nozzle area ratio in  $\tau$ -space, Fig. 2, we obtain the temperature

distributions for the ideal gas and the real gas case. The temperature reaches above 23,000°K with a perfect gas assumption while the real gas effect causes the peak temperature to drop to approximately 16,000°K. As shown in Fig. 3, the pressure drops from the initial value of three atm to about 1.7 atm at the throat. The absorption coefficient  $k_\nu$ , which is the function of density and temperature has two distinct profiles for the two cases. Once the absorption coefficient is known, we can transform the solution into the real space  $x$  by Eq. (3). As shown in Fig. 4, the temperature distributions are somewhat different due to the transformation and the throat is located at about  $x = 3$  cm. With the known thermodynamic conditions in the nozzle, the heat transfer characteristics were then assessed.<sup>12</sup>

Finally, we can proceed to calculate the nozzle contours in the physical space. As one may notice the initial velocity is a function of  $A^*/A_i$  where  $A^*$  is the throat cross-section area. For the example case, the propagation velocity of  $1.09 \times 10^5$  cm/sec requires the nozzle contour to have an area ratio  $A^*/A_i = 0.23$ . In addition, for a known laser power, i.e., 100 kW, the initial cross-sectional area  $A_i$  and hence the complete nozzle size can now be determined (Fig. 4).

### References

- Generalov, N. A., Zimakov, V. P., Kozlov, G. I., Masyukov, V. A., and Raizer, Yu P., "Experimental Investigation of a Continuous Optical Discharge," *Soviet Physics JETP*, Vol. 34, April 1972, p. 763.
- Klosterman, E. L., Byron, S. R., and Newton, J. F., "Laser Supported Combustion Wave Study," Mathematical Sciences Northwest, Inc., Rept. 73-101-3, 1973.
- Lowder, J. E., Leniconi, D. E., Hilton, T. W., and Hull, R. J., "High Energy Pulsed CO<sub>2</sub>-Laser-Target Interaction in Air," *Journal of Applied Physics*, Vol. 44, 1973, p. 2759.
- Jackson, J. P., and Nielsen, P. E., "Role of Radiative Transport in the Propagation of Laser Supported Combustion Waves," *AIAA Journal*, Vol. 12, Nov. 1974, p. 1498.
- Boni, A. A., Cohen, H. D., Meskan, D. A., and Su, F. Y., "Laser Interaction Studies," *Systems, Science and Software*, Rept. 74-2344, Aug. 1974.
- Thomas, P. D., Musal, H. M. and Chou, Y. S., "Laser Beam Interaction - Part II," Lockheed Palo Alto Research Lab., LSCM-D403747, 1974.
- Zel'dovich, Ya. B. and Raizer, Yu. P., *Physics of Shock Waves and High-Temperature Hydrodynamic Phenomena*, Vol. I, Academic Press, 1966, p. 269.
- Yos, J. M., "Transport Properties of Nitrogen, Hydrogen, Oxygen and Air to 30,000°K," AVCO Corporation, Technical Memorandum, RAD-TM-63-7, March 1963.
- Wu, P. K. S. and Pirri, A. N., "Stability of Laser Heated Flows," *AIAA Journal*, Vol. 14, March 1976, pp. 390-392.
- Patch, R. W., "Thermodynamics Properties and Theoretical Rocket Performance of Hydrogen to 100,000°K and  $1.013 \times 10^8$  n/m<sup>2</sup>," NASA SP-3069, 1971.
- Caledonia, G. E., Wu, P. K. S. and Pirri, A. N., "Radiant Energy Absorption Studies for Laser Propulsion," Physical Sciences Inc. TR-20, NASA CR-134809, March 1975.
- Wu, P. K., "Similarity Solution of the Boundary Layer Equations for Laser Heated Flows," *AIAA Journal*, Vol. 14, Nov. 1976 (to be published).

## Entrance Flow in a MHD Channel with Hall and Ion Slip Currents

M. L. Mittal,\* G. H. Masapati,†  
and B. Nageswara Rao†

Indian Institute of Technology, Powai, Bombay, India

THE problem of entry flow in channels has been solved by a number of authors. Targ<sup>1</sup> has analyzed this problem by

Received Aug. 5, 1976; revision received Sept. 22, 1976.

Index category: Plasma Dynamics and MHD.

\*Assistant Professor, Department of Mathematics.

†Junior Research Fellow, Department of Mathematics.

linearizing the inertia terms with the mean velocity. Sparrow et al.<sup>2</sup> improved Targ's method by introducing a stretched coordinate in the flow direction and obtained a closed-form solution for hydrodynamic flows. Using this method, Snyder<sup>3</sup> has analyzed MHD flows in the entrance region of a rectangular channel when the electric current obeys simple Ohm's law without Hall and ion slip currents. He also has given a good bibliography of the earlier work. Recently Chen and Chen<sup>4</sup> and Hwang<sup>5</sup> have considered the entry flow with an arbitrary inlet velocity profile. These studies of entry flow in channels are needed for operational MHD devices like power generators and MHD accelerators. But in these devices, usually the conducting material is a partially ionized gas and, therefore, the Hall and ion slip currents are important for these applications. Saric and Touryan<sup>6</sup> have considered the effect of these currents, using momentum integral method.

In the present analysis, the problem of two-dimensional MHD flow in the entrance region of a rectangular channel is solved with generalized Ohm's law under externally applied, electric field loading conditions. The magnetic Reynolds number is assumed to be small and the induced magnetic field is neglected.

Following the model suggested by Snyder,<sup>3</sup> the equations of motion in the present case are<sup>7</sup>

$$u \frac{\partial u}{\partial x} + w \frac{\partial u}{\partial z} = -\frac{1}{\rho} \frac{\partial p}{\partial x} + \nu \frac{\partial^2 u}{\partial z^2} + \frac{\sigma B_0^2}{\rho \sigma_0^2} [(1 + \beta_e \beta_i) (\frac{E_y}{B_0} - u) + \beta_e (\frac{E_x}{B_0} + v)] \quad (1)$$

$$u \frac{\partial v}{\partial x} + w \frac{\partial v}{\partial z} = -\frac{1}{\rho} \frac{\partial p}{\partial y} + \nu \frac{\partial^2 v}{\partial z^2} + \frac{\sigma B_0^2}{\rho \sigma_0^2} [\beta_e (\frac{E_y}{B_0} - u) - (1 + \beta_e \beta_i) (\frac{E_x}{B_0} + v)] \quad (2)$$

where

$$\sigma_0^2 = (1 + \beta_e \beta_i)^2 + \beta_e^2$$

Multiplying Eq. (2) by  $i = (-1)^{1/2}$  and adding Eq. (1), it becomes

$$u \frac{\partial u'}{\partial x} + w \frac{\partial u'}{\partial z} = -\frac{1}{\rho} (\frac{\partial p}{\partial x} + i \frac{\partial p}{\partial y}) + \nu \frac{\partial^2 u'}{\partial z^2} - \frac{\sigma B_0^2 \alpha_0}{\rho \sigma_0^2} (\frac{i E'}{B_0} + u') \quad (3)$$

where  $u' = u + iv$ ,  $E' = E_x + i E_y$ , and  $\alpha_0 = (1 + \beta_e \beta_i) + i \beta_e$ . Using the method of Sparrow et al.<sup>2</sup> to linearize the inertia terms by the mean velocity  $U$  and a weighting function  $\epsilon(x)$ , Eq. (3) is transformed as

$$\epsilon(x) U \frac{\partial u'}{\partial x} = \Lambda(x) + \nu \frac{\partial^2 u'}{\partial z^2} - \frac{\sigma B_0^2 \alpha_0}{\rho \sigma_0^2} (\frac{i E'}{B_0} + u') \quad (4)$$

where

$$U = \frac{1}{2h} \int_{-h}^h u dz$$

and

$$\frac{1}{2h} \int_{-h}^h v dz = 0$$

Here  $h$  is half the height of the channel. Equation (4) is the same as Eq. (2) of Ref. 3, except that here the functions are